THE JOURNAL OF BIOLOGICAL CHEMISTRY VOL. 289, NO. 20, pp. 13926–13936, May 16, 2014
© 2014 by The American Society for Biochemistry and Molecular Biology, Inc. Published in the U.S.A.

Eukaryotic Translation Initiation Factor eIFiso4G Is Required to Regulate Violaxanthin De-epoxidase Expression in *Arabidopsis*[*]

Received for publication, February 4, 2014, and in revised form, March 21, 2014 Published, JBC Papers in Press, April 4, 2014, DOI 10.1074/jbc.M114.555151

Zhong Chen, Blair Jolley, Christian Caldwell, and Daniel R. Gallie[1]

From the Department of Biochemistry, University of California, Riverside, California 92521-0129

Background: The initiation factor eIFiso4G organizes the assembly of those factors needed to initiate translation of plant mRNAs.

Results: Loss of eIFiso4G results in increased violaxanthin de-epoxidase expression and increased xanthophyll cycle activity.

Conclusion: eIFiso4G is required to maintain VDE expression at an optimal level.

Significance: Of the two isoforms of eIF4G, eIFiso4G is required specifically to support photosynthetic activity.

The eukaryotic translation initiation factor (eIF) 4G is a scaffold protein that organizes the assembly of those initiation factors needed to recruit the 40 S ribosomal subunit to an mRNA. Plants, like many eukaryotes, express two eIF4G isoforms. eIFiso4G, one of the isoforms specific to plants, is unique among eukaryotic eIF4G proteins in that it is highly divergent and unusually small in size, raising the possibility of functional specialization. In this study, the role of eIFiso4G in plant growth was investigated using null mutants for the eIF4G isoforms in *Arabidopsis*. eIFiso4G loss of function mutants exhibited smaller cell, leaf, plant size, and biomass accumulation that correlated with its reduced photosynthetic activity, phenotypes not observed with the eIF4G loss of function mutant. Although no change in photorespiration or dark respiration was observed in the eIFiso4G loss of function mutant, a reduction in chlorophyll levels and an increase in the level of nonphotochemical quenching were observed. An increase in xanthophyll cycle activity and the generation of reactive oxygen species contributed to the qE and qI components of nonphotochemical quenching, respectively. An increase in the transcript and protein levels of violaxanthin de-epoxidase in the eIFiso4G loss of function mutant and an increase in its xanthophyll de-epoxidation state correlated with the higher qE associated with loss of eIFiso4G expression. These observations indicate that eIFiso4G expression is required to regulate violaxanthin de-epoxidase expression and to support photosynthetic activity.

The autotrophic nature of plants relies on their ability to transform absorbed light energy into chemical energy through photosynthesis to fix atmospheric CO_2 into sugars that are used to support growth. Plants use only a fraction of the total light energy they absorb because the capacity of photosynthesis is limited. Levels of light energy exceeding the capacity of photosynthesis can result in the production of reactive oxygen species (ROS),[2] *e.g.* singlet oxygen, superoxide anion, hydroxyl radicals, and H_2O_2 (1, 2). ROS can damage protein subunits and pigments of photosystem II (PSII), resulting in the inactivation of reaction centers, protein degradation, and the inhibition of the subsequent repair mechanisms for the reaction centers (3, 4). Given the potential for light-induced damage, plants have evolved mechanisms to deal with excess absorbed light energy to reduce ROS generation. In addition to quenching as a result of photochemistry (qP), absorbed light energy can be quenched through its dissipation as heat (qE), used in photoinhibition (qI), or re-emitted as light as a consequence of chlorophyll fluorescence.

qE and qI are components of nonphotochemical quenching (NPQ) that limit the generation of ROS by protecting the photosystems from over reduction. Under most growth conditions, qE predominates, is rapidly reversible, and results in the pH-dependent dissipation of excess excitation energy as heat before it is used to generate ROS (5, 6). Under high light conditions or during conditions of stress, *e.g.* drought, ozone exposure, or chilling, qI, which mostly results from photodamage to the reaction centers, can become significant and is only slowly reversible or irreversible (7–10). In addition to qE and qI, NPQ processes include quenching associated with state transition, but this typically contributes little to NPQ and is unlikely to be a significant factor in photoprotection. Thus, NPQ plays an important role in modulating photosynthetic performance (5).

Although many of the components of the photosynthetic machinery are encoded in the chloroplast genome, several regulators of chloroplast gene expression as well as proteins involved in chloroplast development, light harvesting, CO_2 fixation, and NPQ are encoded by nuclear genes. The expression of such proteins relies on the translational machinery present in

[*] This work was supported by National Science Foundation Grant DBI-0820047 and grants from the University of California Agricultural Experiment Station (to D. R. G.).

[1] To whom correspondence should be addressed: Dept. of Biochemistry, University of California, Riverside, CA 92521-0129. Tel.: 951-827-7298; Fax: 951-827-4434; E-mail: drgallie@citrus.ucr.edu.

[2] The abbreviations used are: ROS, reactive oxygen species; PSII, photosystem II; eIF, eukaryotic initiation factor; PFD, photon flux density; VDE, violaxanthin de-epoxidase; NPQ, nonphotochemical quenching; qP, quenching as a result of photochemistry; qE, quenching through dissipation as heat; qI, quenching used in photoinhibition; PABP, poly(A)-binding protein; V, violaxanthin; A, antheraxanthin; Z, zeaxanthin; qPCR, quantitative PCR; RbcL, large subunit of Rubisco; ZE, zeaxanthin epoxidase; Luc, luciferase.

This is an open access article under the CC BY license.

the cytoplasm, which is responsible for synthesizing proteins from nuclear-encoded mRNAs.

The initiation of protein synthesis from nuclear-encoded mRNAs is facilitated through the action of several translation initiation factors that function to recruit the 40 S ribosomal subunit to an mRNA, assist in the recognition of the initiation codon, and promote the assembly of the 80 S ribosome (11–13). Recruitment of the 40 S subunit requires the eukaryotic initiation factor (eIF) 4F, which is composed of eIF4E, eIF4A, and eIF4G. eIF4E functions to bind the 5′-cap structure of an mRNA, eIF4A is an RNA helicase that uses ATP hydrolysis to unwind secondary structure present in the 5′-leader of an mRNA that would otherwise inhibit the scanning of the 40 S subunit in its search for the initiation codon, and eIF4G is a scaffolding protein that interacts with eIF4E, eIF4A, eIF4B (which stimulates the RNA helicase activity of eIF4A), eIF3 (required for 40 S binding to an mRNA), and the poly(A)-binding protein (PABP) (12, 14–16). The interaction of eIF4G with eIF4E bound to the 5′-cap and PABP bound to the poly(A) tail results in the circularization of an mRNA and stimulates translation by promoting 40 S subunit recruitment (17, 18). eIF4B also binds PABP to increase the affinity of PABP for poly(A) RNA (19–21).

As in many eukaryotes, plants express two forms of eIF4F (22). In addition to eIF4F, plants express an eIF4F isoform called eIFiso4F, which is composed of eIFiso4E, eIF4A, and eIFiso4G, although eIF4A typically does not co-purify with either eIF4F or eIFiso4F (23). Like eIF4G, eIFiso4G interacts with eIF4B, eIF4A, and PABP, although eIFiso4G contains only one interaction domain for eIF4B and PABP, whereas eIF4G contains two for each of these partner proteins (24). Among all eukaryotic eIF4G isoforms, however, plant eIFiso4G is unusual in that it is substantially smaller than eIF4G and shares only limited similarity to other eIF4G proteins. For example, wheat eIF4G is 168 kDa, whereas eIFiso4G is just 83–86 kDa, which is smaller than any eIF4G protein in animals or yeast (22, 24). Similarly, two isoforms of eIF4E are present in plants that are referred to as eIF4E and eIFiso4E. As a consequence, eIF4F and eIFiso4F are substantially more divergent from one another than are eIF4F isoforms in other species, suggesting greater functional specialization.

Of those mRNAs analyzed to date, preferential translation by either eIF4G or eIFiso4G has been observed. eIF4G is used to translate mRNAs containing the 5′-leader sequence from tobacco mosaic virus (known as Ω), which functions as a translational enhancer (25). eIF4G also preferentially translates mRNAs containing the 5′-leader sequence from tobacco etch virus, which promotes cap-independent translation (26). Barley α-amylase and oat globulin mRNAs preferentially use eIF4G, whereas *Arabidopsis* HSP21 and alfalfa mosaic virus RNA 4 use eIF4G and eIFiso4G equally well (27). These observations support the notion that eIF4G and eIFiso4G are functionally distinct to some extent and that cellular mRNAs may differ in which isoform they use predominately for their translation.

In *Arabidopsis*, eIF4G is encoded by a single gene (*i.e.* At3g60240), whereas eIFiso4G is encoded by two genes, eIFiso4G1 and eIFiso4G2 (*i.e.* At5g57870 and At2g24050, respectively) (28). Given their role in supporting protein synthesis, loss of a general translational initiation factor might be expected to result in pleiotropic effects or lethality. Interestingly, *eifiso4g1* and *eifiso4g2* loss of function mutants exhibit few visible phenotypes other than a slightly smaller stature in *eifiso4g1* plants, and the eIFiso4G double null, *i.e. eifiso4g1/2*, remains viable, although it has a reduced stature and a slower growth rate (28).

In this study, we investigated the role of eIFiso4G in plant growth. The eIFiso4G loss of function mutant exhibits substantially reduced photosynthetic activity that correlates with a smaller cell, leaf, plant size, and biomass accumulation. Although *eifiso4g1/2* plants exhibit a reduction in stomatal conductance, it was not sufficient to limit internal CO_2 levels because the substomatal CO_2 concentration was not substantially different from the wild-type level. The reduced photochemistry of *eifiso4g1/2* plants was not a result of a change in the level of photorespiration or dark respiration but did correlate with lower chlorophyll levels and elevated levels of the qE and qI components of NPQ, processes that divert absorbed light energy from use in photochemistry. The increase in qE correlated with an increase in the activity of violaxanthin de-epoxidase (VDE), the enzyme responsible for the de-epoxidation of xanthophyll pigments such as violaxanthin (V) and antheraxanthin (A) into zeaxanthin (Z). The increase in VDE activity was a result of its greater expression in the eIFiso4G loss of function mutant, which was reflected at the transcript and protein levels. These results indicate that loss of eIFiso4G expression affects the appropriate regulation of VDE expression, which is not affected by loss of eIF4G expression, and that eIFiso4G expression is important to maintain photosynthetic activity.

EXPERIMENTAL PROCEDURES

Plant Material and Transformation—Col-0 *Arabidopsis* was used throughout this study. After surface sterilization and cold treatment at 4 °C for 4 days in the dark, seeds were planted on 0.25× MS agar plates and grown at 20 °C in a plant growth room supplemented with Sylvania Gro-Lite fluorescent bulbs (Sylvania, Danvers, MA) at a photon flux density (PFD) of 100 μmol photons m^{-2} s^{-1}. For adult plants, seeds were germinated on medium for 1 week and transferred to soil and grown under a 16-h light cycle at 21 °C in a plant growth chamber at 250 PFD. Wild-type *Arabidopsis* was transformed with the firefly luciferase (Luc) transgene under the control of the cauliflower mosaic virus ^{35}S promoter or the *NPQ1* promoter with or without the *NPQ1* 5′leader using the binary vector, pBI121. The primary inflorescences of *Arabidopsis* plants were removed, and the secondary inflorescences were allowed to initiate before infiltration. Inverted plants were dipped into the infiltration medium containing the Aglo1 strain of *Agrobacterium* containing a transgene. Infiltrated plants were kept on their side for 1 day and allowed to continue to flower in an upright position in the same growth room. Seeds of infiltrated plants were collected and screened on 0.25× MS plates containing 50 μg/ml kanamycin and 500 μg/ml vancomycin.

For high light experiments, a Li-6400 portable photosynthesis system (LI-COR, Lincoln, NE) was used for the times indicated. F_o and F_m were measured immediately in dark-adapted

leaves or plants before the high light exposure and at time points during recovery. For the analysis, leaves with similar initial F_v/F_m values were used.

Western Analysis—Protein extracts were resolved using standard SDS-PAGE, and the protein was transferred to 0.22-μm PVDF membrane by electroblotting. Following transfer, the membranes were blocked in 5% milk in TPBS (0.1% Tween 20, 137 mM NaCl, 2.7 mM KCl, 10 mM Na_2HPO_4, 1.4 mM KH_2PO_4, pH 7.4) followed by incubation with antiserum raised against eIF4A, PsbS, or the large subunit of Rubisco diluted 1:1,000 in TPBS with 1% milk for 1.5 h. The blots were then washed twice with TPBS and incubated with goat anti-rabbit horseradish peroxidase-conjugated antibodies (Southern Biotechnology Associates, Inc.) diluted 1:20,000 for 1 h. The blots were washed twice with TPBS, and the signal was detected using chemiluminescence (Amersham Biosciences).

Chlorophyll Measurements—Chlorophyll *a* and *b* were measured spectrophotometrically as described (29). Leaf samples were ground in liquid nitrogen and extracted with 90% (v/v) acetone. The absorbance at 664 and 647 nm was determined and used to calculated chlorophyll *a* and *b* content by the equations: Chl $a = 11.93A_{664} - 1.93A_{647}$ and Chl $b = 20.36A_{647} - 5.50A_{664}$, respectively. Each experiment was repeated two or three times, and representative results are presented.

Xanthophyll pigments were extracted with 100% acetone under dim light and were separated on a Spherisorb ODS-1 column (Alltech) as described (30), using solvent A-1: acetonitrile:methanol:0.1 M Tris-HCl, pH 7.5 (72:8:3), and solvent B: methanol:hexane (4:1). Pigments were identified and quantified by the retention time and amount of standards using a photodiode array detector.

Gas Exchange and Fluorescence Measurements—Gas exchange and fluorescence measurements were performed using LI-COR Li-6400 portable photosynthesis system with LI-6400-40 leaf chamber, a relative humidity of 50%, and ambient level of CO_2. Fluorescence measurements were taken using overnight dark-adapted leaves. At the start of each experiment, the leaf was exposed to 2 min of far-red illumination (1 PFD) for the determination of F_o (minimum fluorescence in the dark-adapted state). Saturating pulses (0.8 s of 7000 PFD) were applied to determine the F_m or F_m' values. Actinic light, consisting of 90% of red light ($\lambda = 630 \pm 20$ nm) and 10% blue light ($\lambda = 470 \pm 20$ nm) was provided by light emission diode sources. F_s is the steady fluorescence yield during actinic illumination. F_o' (minimum fluorescence in the light-adapted state) was determined in the presence of far-red ($\lambda = 740$ nm) light after switching off the actinic light. A total of four to six samples were measured in each experiment. All data presented were calculated from at least three independent measurements. Conventional fluorescence nomenclature was used (31). NPQ was calculated from $(F_m - F_m')/F_m'$, ϕPSII from $(F_m' - F_s')/F_m'$, qP from $(F_m' - F_s)/(F_m' - F_o')$.

For the determination of NPQ_f and NPQ_s, F_m^o was recorded from dark-adapted leaves, following which, leaves were exposed to 1200 PFD actinic light for 10 min, and F_m' was recorded at the end of light period. F_m was continuously recorded for 45 min at 1-min intervals immediately after the actinic light was turned off. NPQ_f and NPQ_s were calculated as described (31) using $NPQ_s = (F_m^o - F_m^r)/F_m^r$ and $NPQ_f = (F_m^o/F_m') - (F_m^o/F_m^r)$. F_m^r was calculated from the extrapolation of $\log(F_m)$ to the time point where the actinic light was switched off.

H_2O_2 Assay—Foliar H_2O_2 concentrations were determined as described (32), based on the peroxide-mediated oxidation of Fe^{2+}, followed by the reaction of Fe^{3+} with xylenol orange (*o*-cresolsulfonephtalein 3′-3′-bis-[methyliminol] diacetic acid, sodium salt). Protein was removed from the leaf extract by adding an equal volume of 25 mM HCl. Protein-depleted extract was mixed with an equal volume of 2× assay reagent (500 μM ammonium ferrous sulfate, 2200 mM $HClO_4$, 200 μM xylenol orange, and 200 mM sorbitol). Absorbance of the Fe^{3+}-xylenol orange complex (A_{560}) was detected after 45 min. The specificity for H_2O_2 was tested by removing H_2O_2 from the reaction mixture using catalase prior to protein removal. Standard H_2O_2 curves were obtained for each independent experiment by adding various amounts of H_2O_2 to 500 μl of assay reagent.

qPCR Analysis—Plant material was frozen in liquid nitrogen and ground to a fine powder, and 100 mg was resuspended in 1 ml of TRIzol® reagent (Invitrogen). Following centrifugation, the supernatant was extracted with 200 μl of chloroform and centrifuged to separate the phases. RNA was precipitated from the aqueous phase using isopropyl alcohol, and the RNA pellet was washed with 75% ethanol and resuspended in RNase-free H_2O. 1 μg of RNA was used to obtain the first-strand cDNA by Omniscript RT kit (Qiagen) in a 20-μl reaction. The qPCR analysis was performed using a iQ5 real time PCR detection system (Bio-Rad) in 25-μl reactions containing 1× SYBR Green SuperMix 500 nM forward and reverse primers and 10 ng of cDNA. Reactions were carried out using the following conditions: 95 °C for 5 min (1 cycle) and 95 °C for 30 s, 55 °C for 30 s, and 72 °C for 30 s (35 cycles). To detect the presence of Luc, a forward primer, Luc-F1 (5′-CCGTTGTTGTTTTGGAGCACGGAAA-3′), and a reverse primer, Luc-R1 (5′-GATCTCTCTGATTTTTCTTGCGTCGAG-3′), were used. Protein phosphatase PP2A (At1g13320) was used as the reference gene for the quantitation of *Luc* expression in *Arabidopsis* leaves. To detect the expression of PP2A, a forward primer, PP2A-FW (5′-AGTATCGCTTCTCGCTCCAG-3′). and a reverse primer, PP2A-RV (5′-GTTCTCCACAACCGCTTGGT-3′), were used. The efficiency of PCR was determined by five 10-fold serial dilutions of the template DNAs in triplicate.

RESULTS

eIFiso4G Is Required to Support Photosynthetic Activity—eIF4G is encoded by a single gene (*i.e.* At3g60240), whereas eIFiso4G is encoded by *eIFiso4G1* and *eIFiso4G2* (*i.e.* At5g57870 and At2g24050, respectively). To determine the extent to which each eIF4G isoform affects plant growth and development, SALK T-DNA insertion knock-out lines were identified for eIF4G, eIFiso4G1, and eIFiso4G2. Knock-out lines were also identified for eIF4E and eIFiso4E. Loss of eIF4G or eIFiso4G2 expression had no discernible effect on growth (data not shown). Loss of eIFiso4G1 expression resulted in only a slight reduction in plant stature, but the *eifiso4g1/2* double mutant was substantially smaller than either single mutant or WT plants as previously reported (28). Combining the *eif4g*

mutation with *eifiso4g1*, resulting in an *eif4g/eifiso4g1* double mutant, resulted in slight reduction in plant stature but less so than observed for the *eifiso4g1/2* double mutant (data not shown). Loss of eIF4E expression from At4g18040, which is the predominantly expressed member of the eIF4E gene family (*i.e.* At4g18040, At1g29590, and At1g29550), had no effect on plant growth. Although eIFiso4E is expressed by a single gene (*i.e.* At5g35620), loss of eIFiso4E expression had no effect on plant growth (data not shown).

Because the *eifiso4g1/2* double mutant grew at a slower rate than WT plants (28), growth of *eifiso4g1/2* plants was compared with WT plants at a similar developmental stage. Just prior to the appearance of the inflorescence, *eifiso4g1/2* plants were substantially smaller than the wild type whether grown at low, *i.e.* 50 μmol photons m^{-2} s^{-1} (PFD), or moderate (250 PFD) light (Fig. 1*A*). *eifiso4g1/2* adult leaves were 37.7 or 51.7% the size of adult WT leaves when grown at low or moderate light, respectively (Table 1). *eifiso4g1/2* leaf size was smaller than the wild type for both the juvenile and adult stage (Fig. 1, *B* and *C*, respectively) as was root growth (Fig. 1*D*). *eifiso4g1/2* cell size in adult leaves was 42.0% (low light) or 53.6% (moderate light) of that in WT leaves with only a small reduction in cell number per leaf (Table 1). Little change in the stomatal index (*i.e.* the ratio of stomata per epidermal cell) was observed, although *eifiso4g1/2* plants exhibited a substantial reduction in the number of trichomes (Table 1). Following flowering, the inflorescence of *eifiso4g1/2* plants was substantially smaller than in WT plants (Fig. 1*E*).

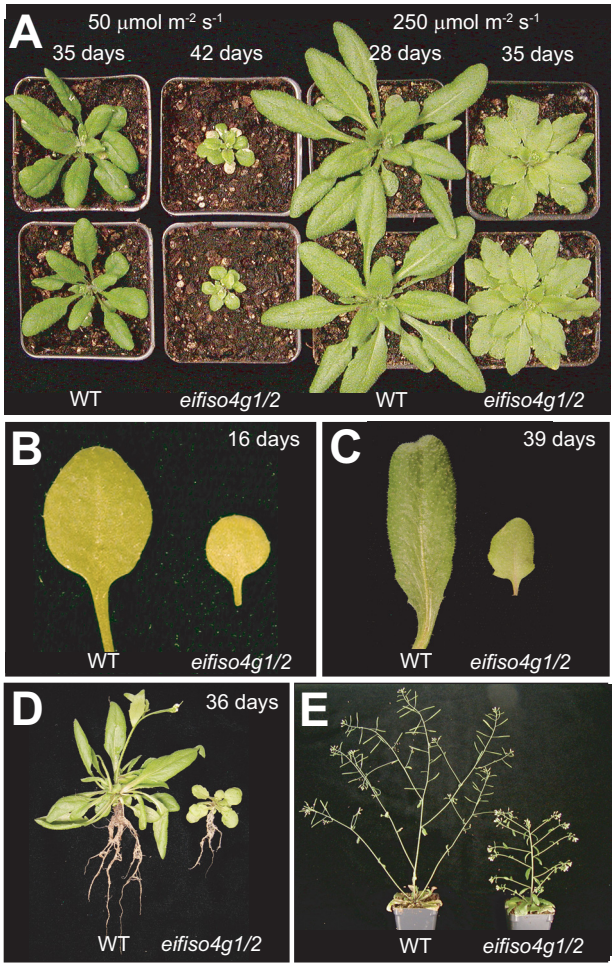

FIGURE 1. **Growth phenotypes of initiation factor mutants.** WT and the *eifiso4g1/2* mutant were grown the same developmental stage within each panel. *A*, plants were grown at the light level indicated to approximately the appearance of the inflorescence. *B–E*, plants were grown at 250 PFD. *B*, juvenile leaves of 16-day-old plants. *C*, adult leaves of 39-day-old plants. *D*, adult plants at flowering. *E*, the inflorescence of flowering plants.

The chlorophyll *a* and *b* content of *eifiso4g1/2* adult leaves was reduced relative to WT plants, which accounted for their pale green appearance (28). To examine whether the relative chlorophyll content of *eifiso4g1/2* was affected by light intensity, the mutant and WT plants were grown at different light levels. A similar relative reduction in chlorophyll *a* and *b* content in *eifiso4g1/2* leaves was observed regardless of whether the plants were grown at extremely low (25 PFD), low (50 PFD), moderate (250 PFD), or high (1250 PFD) light levels (Fig. 2*A*). *eifiso4g1/2* plants grown at 250 PFD that were then exposed to either 1075 PFD or full sun for 2 h exhibited a slightly greater relative reduction in chlorophyll *a* and *b* content than observed for WT plants, suggesting greater photosensitivity. The reduction in chlorophyll content in *eifiso4g1/2* leaves was accompanied by a reduction in the level of light-harvesting complex II protein at each light level tested (Fig. 2*B*).

eifiso4g1/2 plants exhibited substantially lower fresh weight and dry weight (Table 2). The reduced fresh weight was partly explained by the smaller water content as a consequence of its smaller cell size, but its lower dry weight demonstrates a substantial reduction in biomass accumulation. To examine whether a reduction in photosynthetic activity might account for the reduced stature of *eifiso4g1/2*, the rate of CO_2 assimilation was measured in adult leaves at the same developmental stage as WT plants. Correlating with its reduced biomass accumulation, the rate of CO_2 assimilation in *eifiso4g1/2* was approximately half of the WT level (Table 2). When measured under ambient oxygen, this rate represents net CO_2 assimilation, which is the rate resulting from photochemistry minus CO_2 produced from photorespiration and dark respiration. To

TABLE 1
eIFiso4G regulates leaf and cell size

	25 μmol photons/m^2/s			250 μmol photons/m^2/s		
	Col-0	*eifiso4g1/2*	*t* test	Col-0	*eifiso4g1/2*	*t* test
Leaf size (mm^2)[a]	281 ± 25.3	106 ± 9.3	$p < 0.001$	333 ± 34.2	172 ± 18.3	$p < 0.001$
Cell size (μm^2)	2964 ± 364	1244 ± 221	$p < 0.001$	3321 ± 468	1779 ± 231	$p < 0.001$
Epidermal cells/leaf	94,940	85,414		100,189	96,482	
Stomatal index[b]	0.307 ± 0.019	0.297 ± 0.014	$p = 0.162$	0.311 ± 0.014	0.314 ± 0.017	$p = 0.686$
Trichome density[c]	4.85 ± 0.02	7.11 ± 0.06	$p < 0.001$	3.77 ± 0.01	6.35 ± 0.04	$p < 0.001$

[a] Adult leaves from 21-day-old plants grown at 250 PFD.
[b] Number of stomata per epidermal cell (*i.e.* stomata + epidermal cells).
[c] Number of trichomes/1000 epidermal cells.

examine whether *eifiso4g1/2* may have a higher level of photorespiration, the rate of CO_2 assimilation was measured under 2% oxygen, which largely represses photorespiration. As expected, repressing photorespiration resulted in a higher rate of CO_2 assimilation, but the rate in *eifiso4g1/2* leaves remained approximately half of the WT level (Table 2). The compensation point serves as a measure of photorespiration and dark respiration when performed under ambient oxygen levels or a measure of dark respiration specifically when performed under 2% oxygen. The compensation point of *eifiso4g1/2* leaves under ambient oxygen levels was similar to that in WT leaves but moderately higher under 2% oxygen, suggesting that the reduced photosynthetic activity of *eifiso4g1/2* is not a consequence of increased photorespiration, and its increase in dark respiration can account for only a small fraction of its reduced photosynthetic activity.

To examine whether the reduced photosynthetic activity of the *eifiso4g1/2* mutant involved a reduction in the level of ribulose bisphosphate carboxylase (Rubisco), the enzyme responsible for CO_2 fixation, Western analysis of the large subunit of Rubisco (RbcL) was performed. The level of RbcL was actually higher in *eifiso4g1/2* relative to WT leaves (Fig. 3). An increase in the level of RbcL was also observed in the *eif4g/eifiso4g1* double mutant and to a lower extent in *eifiso4g2* leaves with no change in the *eif4e*, *eifiso4e*, *eif4g*, or *eifiso4g2* mutants. Consequently, the lower photosynthetic activity of the *eifiso4g1/2* mutant was not due to a reduction in RbcL expression. No substantial change in the level of eIF4A, a partner protein of eIF4G and eIFiso4G, was observed in any of the mutants. No substantial change in the level of PsbS, a nuclear-encoded, thylakoid lumen-localized protein involved in the qE component of NPQ, was observed in any of the mutants.

The eifiso4g1/2 Mutant Exhibits Elevated Nonphotochemical Quenching—NPQ, the process of dissipating excess absorbed light energy as heat, protects the photosystems from over-reduction and regulates photosynthetic performance (5). Because NPQ competes with photosynthesis for absorbed light energy,

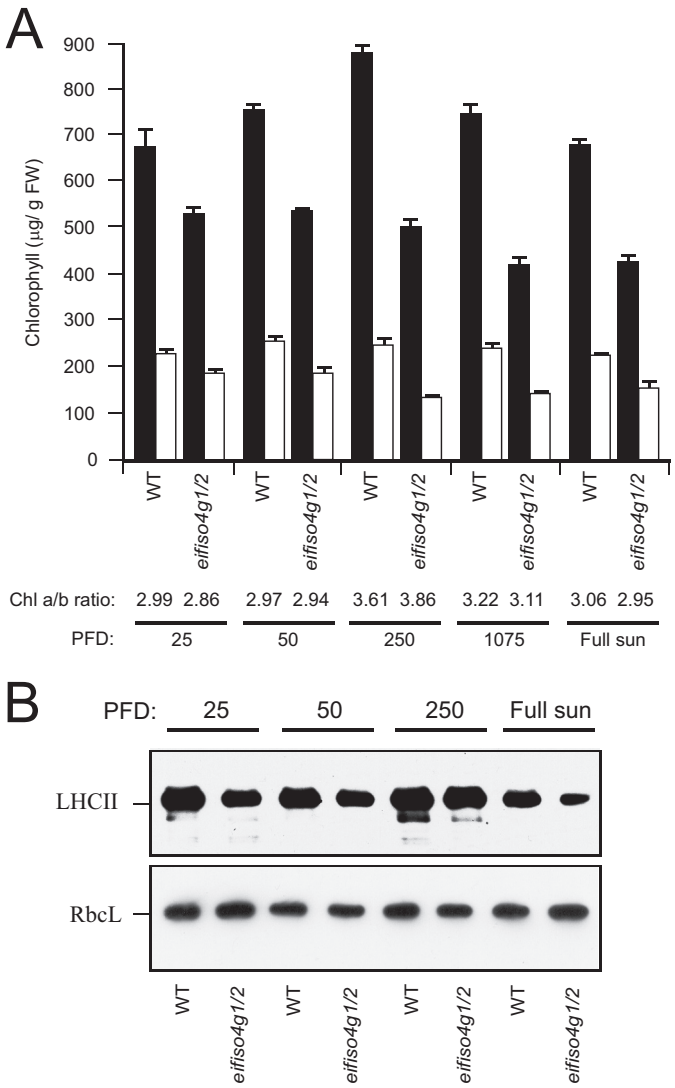

FIGURE 2. **eIFiso4G expression regulates chlorophyll content.** *A*, WT and the *eifiso4g1/2* mutant were grown to a similar developmental stage at the light level (PFD) indicated, and the levels of chlorophyll *a* and *b* were measured in adult leaves. The ratio of chlorophyll a and *b* (*Chl a/b*) indicated below the histograms. *B*, light-harvesting complex II (*LHCII*) relative to normalized RbcL protein levels was measured by Western analysis of the same leaf samples as indicated.

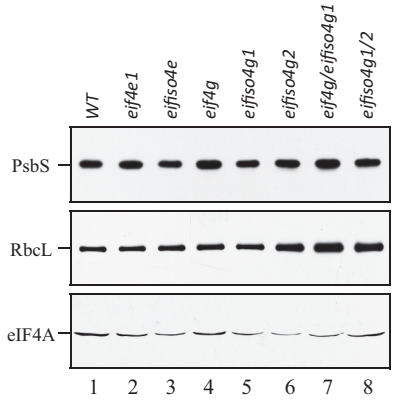

FIGURE 3. **Rubisco and PsbS protein levels in initiation factor mutants.** WT, *eif4e*, *eifiso4e*, *eif4g*, *eifiso4g1*, *eifiso4g2*, *eif4g/eifiso4g1*, and *eifiso4g1/2* mutants were grown at a PFD of 250 PFD for to a similar developmental stage, and the levels of PsbS and RbcL were determined using Western analysis and compared with eIF4A on a fresh weight basis.

TABLE 2

eIFiso4G regulates CO_2 assimilation and biomass accumulation

	Col-0	*eifiso4g1/2*	*t* test
CO_2 assimilation under ambient oxygen (μmol $CO_2/m^2/s/g$ FW)[a]	650 ± 276	335 ± 36.3	$p < 0.001$
CO_2 assimilation under 2% oxygen (μmol $CO_2/m^2/s/g$ FW)[a]	841 ± 274	456 ± 31.1	$p < 0.001$
Compensation point (Ci) under ambient oxygen (μmol CO_2/mol)[b]	63.0	65.1	
Compensation point (Ci) under 2% oxygen (μmol CO_2/mol)[b]	14.8	19.2	
Fresh weight (g)[b]	1.72 ± 0.46	0.131 ± 0.053	$p < 0.001$
Dry weight (g)[b]	0.14 ± 0.04	0.013 ± 0.005	$p < 0.001$

[a] Measured from plants grown to the same developmental stage at 250 PFD. FW, fresh weight.
[b] Plants grown for 28 days at 250 PFD.

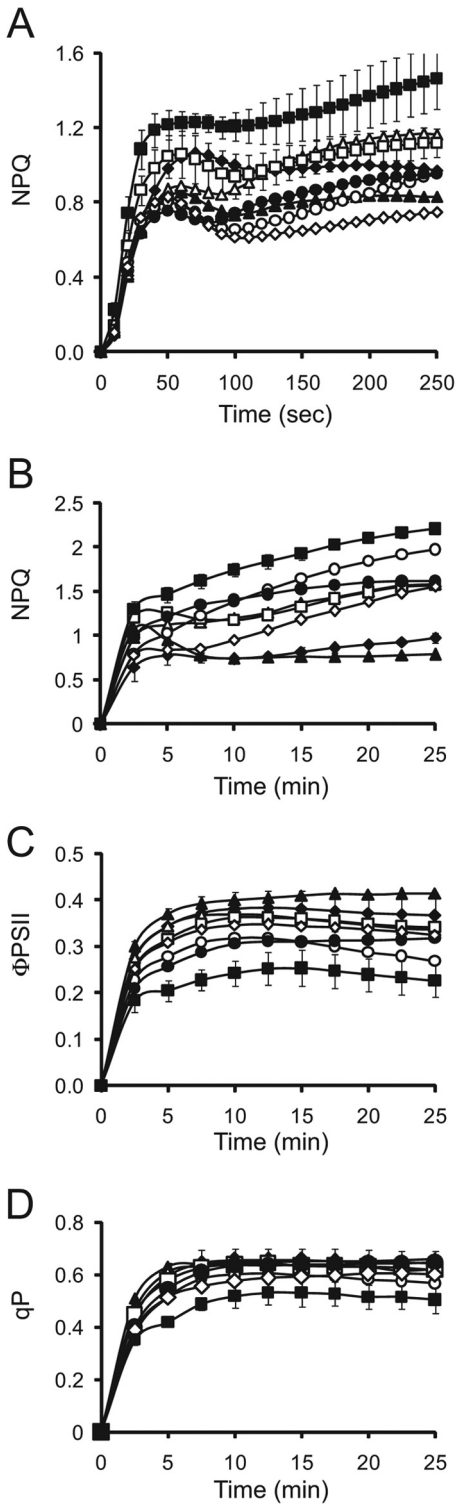

FIGURE 4. **The *eifiso4g* loss of function mutant exhibits increased induction of nonphotochemical quenching.** *A* and *B*, rapid (*A*) and slow (*B*) induction of NPQ was measured in dark-adapted WT (*filled diamonds*), *eif4e* (filled triangles), *eifiso4e* (*open triangles*), *eif4g* (*open squares*), *eifiso4g1* (*open circles*), *eifiso4g2* (*filled circles*), *eif4g/eifiso4g1* (*open diamonds*), and *eifiso4g1/2* (*filled squares*) plants grown at 250 PFD to a similar developmental stage and exposed to 500 PFD. *C* and *D*, quantum yield of PSII (*C*, ϕPSII) and photochemical quenching (*D*, qP) were measured simultaneously with the slow induction of NPQ. Eight replicates were assayed for each line in *A*, and four or five replicates were assayed for each line in *B–D* with the average and standard error reported.

TABLE 3

NPQ, ΦPSII, and qP of initiation factor mutants

Measurements are from Fig. 4 from plants grown to the same developmental stage at 250 PFD and exposed to 500 PFD.

Mutant	NPQ at 20 s	NPQ at 10 min	ΦPSII at 10 min	qP at 10 min
WT	0.409 ± 0.071	0.736 ± 0.035	0.381 ± 0.038	0.653 ± 0.047
eif4e	0.405 ± 0.072	0.743 ± 0.020	0.400 ± 0.014	0.646 ± 0.020
eifiso4e	0.417 ± 0.035	1.195 ± 0.149	0.369 ± 0.033	0.638 ± 0.042
eif4g	0.566 ± 0.099	1.177 ± 0.263	0.363 ± 0.037	0.637 ± 0.043
eifiso4g1	0.479 ± 0.111	1.380 ± 0.025	0.318 ± 0.020	0.599 ± 0.020
eifiso4g2	0.435 ± 0.056	1.407 ± 0.062	0.306 ± 0.031	0.635 ± 0.035
eif4g/eifiso4g1	0.458 ± 0.086	0.948 ± 0.222	0.345 ± 0.030	0.575 ± 0.046
eifiso4g1/2	0.742 ± 0.088	1.746 ± 0.073	0.242 ± 0.027	0.519 ± 0.044

an increase in NPQ may account for the reduced photosynthetic activity of the *eifiso4g1/2* mutant. To examine this possibility, the rate of induction of NPQ was measured in dark-adapted *eifiso4g1/2* plants exposed to moderately high but nonsaturating light (500 PFD). Fast NPQ induction kinetic analysis of WT leaves revealed that NPQ increased rapidly in the first 1–2 min following light exposure and then dropped to a steady-state level (Fig. 4*A*). NPQ was induced in the *eifiso4g1/2* mutant faster and to a higher level than observed in WT leaves (Fig. 4*A*), which was observed during the early induction of NPQ, as well as after longer exposures to light (Table 3). Following the full induction of photochemistry, the level of NPQ in the *eifiso4g1/2* mutant continued to increase, which was greater than that observed for any of the other mutants (Fig. 4*A*). Examination of the induction of NPQ over a longer period revealed that NPQ continued to increase for at least 25 min, whereas NPQ remained at its steady-state level following its initial increase (Fig. 4*B*). No other mutant exhibited an elevated induction of NPQ to the extent observed for the *eifiso4g1/2* mutant. The quantum efficiency of photosystem II (ΦPSII) was also lowest in *eifiso4g1/2* plants (Fig. 4*C* and Table 3) and was accompanied by a reduction in photochemistry (Fig. 4*D* and Table 3). An aberrantly high level of NPQ was observed in the *eifiso4g1/2* mutant over a range of light intensities with the exception of light levels below the level to which the mutant was grown, *i.e.* 250 PFD (Fig. 5*A*). The elevated level of NPQ was accompanied by a reduction in ΦPSII (Fig. 5*B*) and photochemistry (Fig. 5*C*) relative to the WT. These results indicate that a loss of eIFiso4G causes an increase in NPQ as a function of the level of light used and length of light exposure. The higher induction of NPQ in *eifiso4g1/2* correlated with a lower level of photochemistry and may contribute to its reduced photosynthetic activity.

The faster initial induction of NPQ in the *eifiso4g1/2* mutant suggested a greater qE component of NPQ, whereas the continued increase in NPQ following prolonged exposure to light suggested a greater qI component of NPQ. NPQ is composed of a fast relaxing component (*i.e.* NPQ_f) and a slow relaxing component (*i.e.* NPQ_s), which are typically measured during recovery from exposure to high light. NPQ_f is largely due to high energy state quenching (qE), which is rapidly reversible and relaxes within minutes following transfer to darkness, whereas NPQ_s is often a result of photoinhibition caused by damage that requires time to repair. NPQ_f and NPQ_s were measured in *eifiso4g1/2*, and WT leaves at a similar developmental stage following exposure to high light (*i.e.* 1200 PFD). Higher levels of

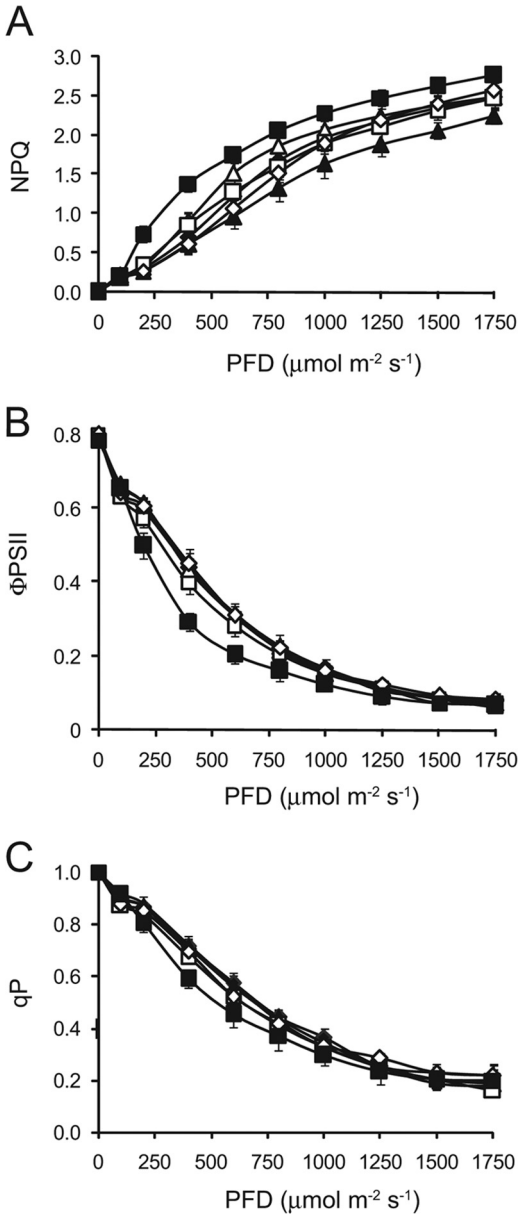

FIGURE 5. **Increased nonphotochemical quenching in the *eifiso4g* mutant as a function of light intensity.** NPQ (*A*) and quantum yield (B) of PSII (ϕPSII) and photochemical quenching (*C*, qP) were measured in dark-adapted WT (*filled diamonds*), *eif4e* (filled triangles), *eifiso4e* (*open triangles*), *eif4g* (*open squares*), *eif4g/eifiso4g1* (*open diamonds*), and *eifiso4g1/2* (*filled squares*) plants grown at 250 PFD to a similar developmental stage and exposed to a range of light intensities. Four to five replicates were assayed for each line with the average and standard error reported.

TABLE 4

Loss of eIFiso4G expression results in photosensitivity

Measurements are from plants grown to the same developmental stage at 250 PFD and exposed to 1200 PFD for 10 min.

	Col-0	*eifiso4g1/2*	*t* test
NPQ	2.13 ± 0.11	2.57 ± 0.08	$p < 0.005$
NPQ_s	0.36 ± 0.02	0.60 ± 0.12	$p < 0.005$
NPQ_f	1.77 ± 0.09	1.96 ± 0.10	$p < 0.05$

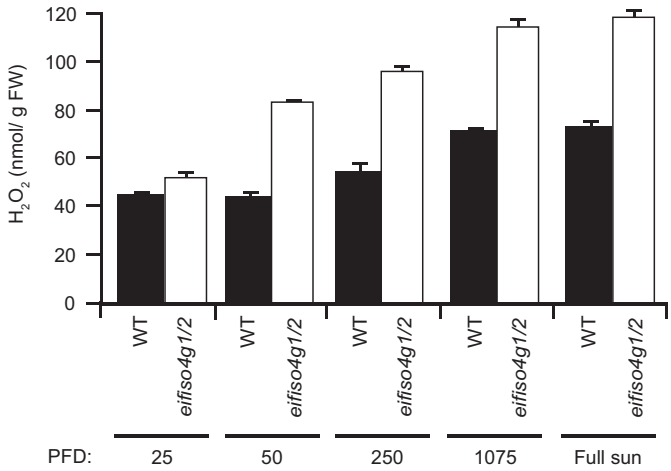

FIGURE 6. **Oxidative load increases in the *eifiso4g1/2* mutant.** WT and the *eifiso4g1/2* mutant were grown to a similar developmental stage at the light level (PFD) indicated, and the level of H_2O_2 was measured in adult leaves. Three replicates were assayed for each line, and the average and standard error were reported.

NPQ_f and NPQ_s were observed in *eifiso4g1/2* relative to WT leaves as was the total level of NPQ (Table 4). Therefore, the increase in NPQ in the *eifiso4g1/2* mutant is due to increases in NPQ_f and NPQ_s, indicating that qE- and qI-related processes both contribute to the higher total NPQ of the mutant.

To examine whether loss of eIFiso4G expression affects ROS, which can accompany an increase in qI-related processes, the level of H_2O_2 was used as a measure of the oxidative load in WT and mutant plants. As expected, the level of H_2O_2 was lowest in WT leaves of plants grown under low light (*i.e.* 25 PFD) and increased with light intensity (Fig. 6). The level of H_2O_2 in *eifiso4g1/2* leaves was similar to the WT when grown under low light (*i.e.* 25 PFD) but increased disproportionately at higher light intensities (Fig. 6). These results suggest that the oxidative load in *eifiso4g1/2* is significantly elevated at light levels greater than 25 PFD. Collectively, these results demonstrate that a loss of eIFiso4G expression reduces photochemistry and increases the qE and qI components of NPQ, ROS generation, and dark respiration.

Loss of eIFiso4G Results in Increased Violaxanthin De-epoxidase Expression—Induction of qE is accompanied by de-epoxidation of violaxanthin into zeaxanthin (or antheraxanthin) as part of the xanthophyll cycle (Fig. 7*A*). Xanthophyll pigments have been implicated in protective processes other than NPQ and have been suggested to scavenge ROS such as $^1O_2$ (33). Zeaxanthin (Z) and antheraxanthin (A) may be superior photoprotectors than violaxanthin (V), whereas the latter may be a better light-harvesting accessory pigment (33, 34). Therefore, conversion of V to Z reduces the amount of V available to transfer excitation energy to the reaction center but increases the amount of Z (or A) that contributes to the qE component of NPQ and to scavenging $^1O_2$. The observation that NPQ was induced at a faster rate in the *eifiso4g1/2* mutant relative to the WT suggested the possibility of an increase in the de-epoxidation state in the mutant. To examine this, the de-epoxidation state of the xanthophyll pigments was examined in *eifiso4g1/2* and WT leaves when dark or light-adapted. Because VDE de-epoxidizes V to A and Z in response to light (35), V predominates in fully dark-adapted plants, whereas A and Z are generated as a function of light intensity (Fig. 7*A*). As expected, no A or Z was present in *eifiso4g1/2* and WT leaves (Fig. 7*B*). Following light adaptation to 100 PFD, representing a low level of light

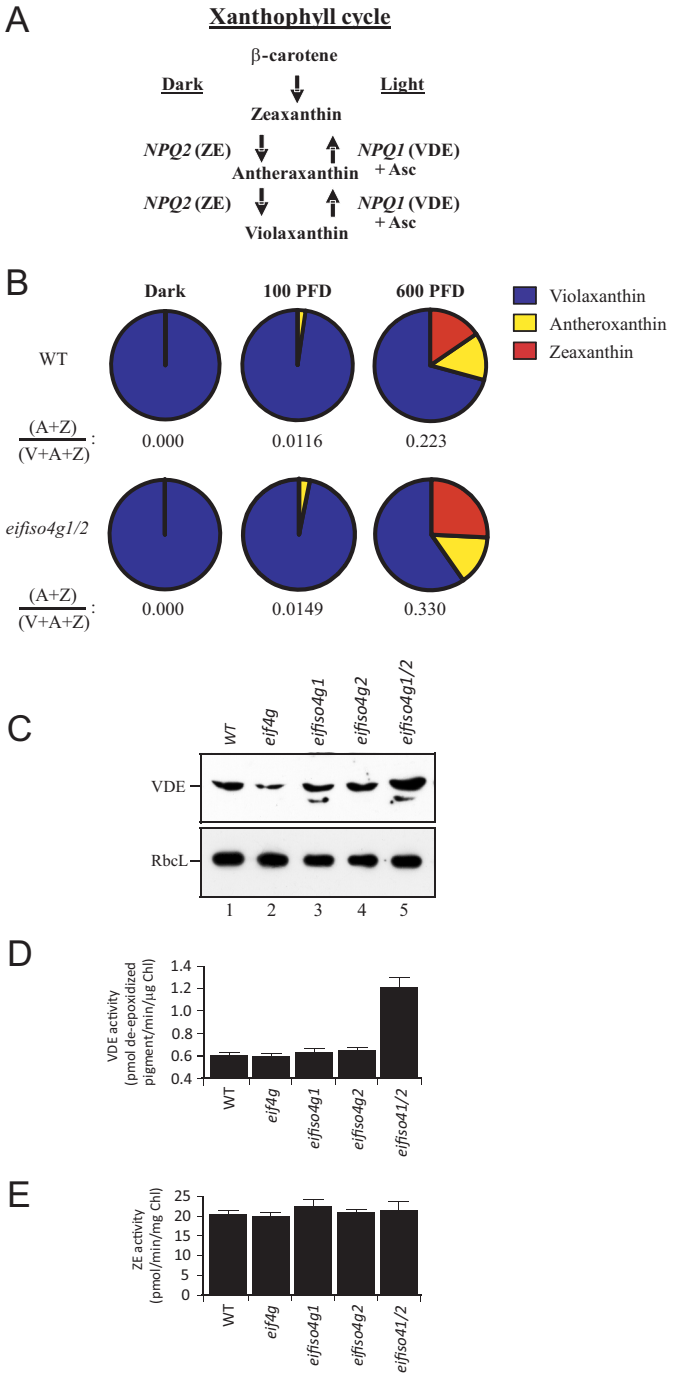

FIGURE 7. **Loss of eIFiso4G expression results in an increase in VDE expression and de-epoxidation.** *A*, the xanthophyll cycle. *NPQ1* encodes violaxanthin de-epoxidase (VDE) whereas *NPQ2* encodes ZE. *B*, xanthophyll pigments were isolated from leaves of plants grown at 100 PFD that were either dark-adapted for 16 h, maintained under 100 PFD, or exposed to 600 PFD for 60 min. Xanthophyll pigments were quantitated by HPLC and normalized to chlorophyll *a*. The de-epoxidation status, *i.e.* (A + Z)/(V + A + Z), was determined from the amounts of V, A, and Z and is included below each pie chart. *C*, VDE relative to normalized RbcL protein levels were measured by Western analysis in adult leaves of the mutants indicated. *D* and *E*, VDE (*D*) and ZE enzyme (*E*) activities were measured in adult leaves of the mutants indicated.

at which the plants were grown, de-epoxidation of V to A but not to Z was observed (Fig. 7*B*). The de-epoxidation state, *i.e.* the fraction of xanthophyll pigments present in a de-epoxidized state, in WT plants increased from a value of 0 in the dark-adapted state to 0.0116 (Fig. 7*B*). The de-epoxidation state in *eifiso4g1/2* was significantly higher (Fig. 7*B*). When dark-adapted plants were exposed to 600 PFD, representing a high level of light for plants grown at 100 PFD, conversion of V to A and Z was observed, and the de-epoxidation state in *eifiso4g1/2* was significantly higher than in WT leaves (Fig. 7*B*). No substantial change in lutein or neoxanthin was observed in *eifiso4g1/2* (data not shown). These results demonstrate an increase in the de-epoxidation state in the *eifiso4g1/2* mutant in response to light exposure that is consistent with its faster initial induction of NPQ.

An increase in the de-epoxidation state could result from increased VDE activity or lower zeaxanthin epoxidase (ZE) activity, which catalyzes the epoxidation of Z to A and then to V, *i.e.* the reverse of VDE activity (Fig. 7*A*). Therefore, the activity of VDE and ZE was measured from thylakoids isolated from WT, *eif4g*, *eifiso4g1*, *eifiso4g2*, and *eifiso4g1/2* leaves. The assay for VDE involves an *in vitro* pH-mediated activation of its activity, mimicking the light-mediated acidification of the thylakoid lumen where VDE resides. As a consequence, the VDE assay measures the maximum capacity of VDE activity, not necessarily the level of activation achieved *in vivo*, because this depends on the magnitude of the transthylakoid membrane pH gradient established. The maximum level of VDE activity measured in *eifiso4g1/2* thylakoids was substantially higher than that measured in WT, *eif4g*, *eifiso4g1*, or *eifiso4g2* plants (Fig. 7*D*). In contrast, little change in ZE activity was observed (Fig. 7*E*), suggesting that the increase in VDE activity was solely responsible for the increase in de-epoxidation in *eifiso4g1/2*. Western analysis revealed a higher level of VDE protein in *eifiso4g1/2* relative to WT, *eif4g*, *eifiso4g1*, or *eifiso4g2* plants (Fig. 7*C*), consistent with the increase in VDE activity observed for *eifiso4g1/2*. qPCR analysis of *NPQ1* mRNA, which encodes VDE, revealed a 5.28-fold increase in the transcript in *eifiso4g1/2* relative to WT, supporting the observed increase in VDE protein and activity.

The increase in VDE expression may be a result of an increase in *NPQ1* promoter activity or *NPQ1* transcript stability/translatability. To distinguish between these possibilities, the *NPQ1* promoter was fused to the firefly luciferase (Luc) reporter, *i.e.* *NPQ1*::Luc (Fig. 8*A*). In a second construct, the *NPQ1* promoter and its 5′-UTR was fused to the Luc reporter, *i.e.* *NPQ1*::*NPQ1 5′-UTR*-Luc. Following transformation of WT *Arabidopsis*, lines homozygous for the *NPQ1*::Luc and *NPQ1*::*NPQ1 5′-UTR*-Luc constructs were isolated. *Arabidopsis* containing the cauliflower mosaic virus 35S promoter driving expression of luciferase was used as a control. Each construct was introduced into *eifiso4g1/2* through crosses with WT lines containing these constructs and progeny homozygous for each transgene, and the *eifiso4g1/2* mutations were isolated. *NPQ1* promoter activity as measured by luciferase activity from the *NPQ1*::Luc construct was reduced in light-adapted *eifiso4g1/2* leaves more than 4-fold relative to the same construct in WT leaves (Fig. 8*B*). Similarly, luciferase activity from the 35S::Luc construct was lower in *eifiso4g1/2* relative to WT (Fig. 8*B*). That luciferase activity resulting from the 35S::Luc construct was reduced to a greater extent than it was from the

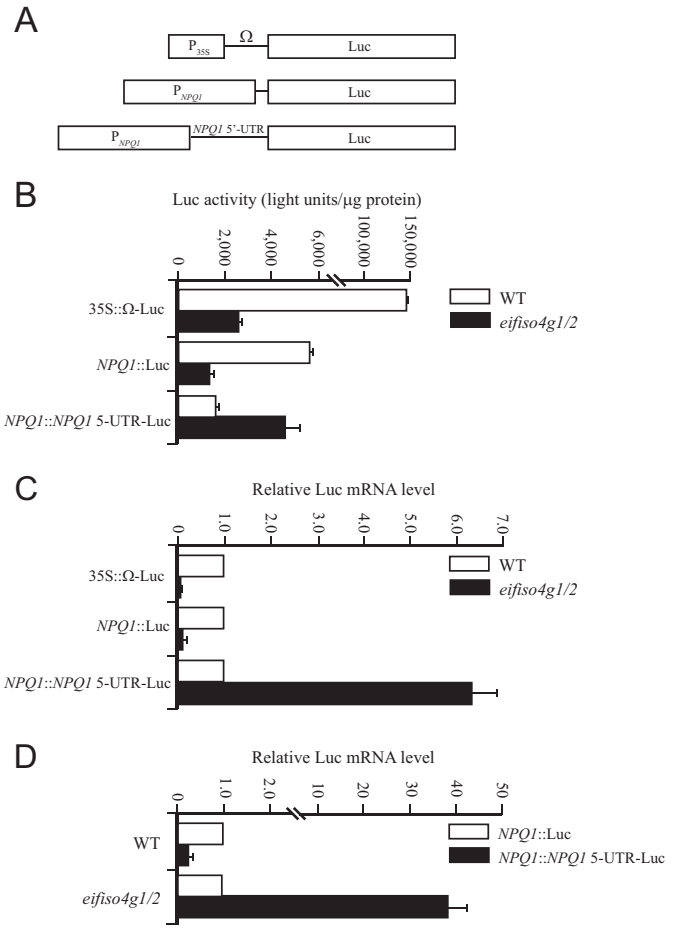

FIGURE 8. **Loss of eIFiso4G results in an increase in VDE expression.** *A*, the 35S::Luc, *NPQ1*::Luc, and *NPQ1*::*NPQ1* 5′-UTR-Luc constructs used to generate transgenic *Arabidopsis* WT and *eifiso4g1/2* lines. *B*, luciferase expression from each construct was measured in adult leaves of each line grown at 100 PFD. *C*, qPCR analysis of Luc mRNA in the same leaf samples as indicated. *D*, the qPCR data are presented as the level of Luc transcript from the *NPQ1*::*NPQ1* 5′-UTR-Luc construct relative to that from the *NPQ1*::Luc construct in the WT and *eifiso4g1/2* lines.

NPQ1::Luc construct in *eifiso4g1/2* leaves suggests that *NPQ1* promoter activity is less affected than is the 35S promoter by a loss of eIFiso4G expression. Luciferase activity from the *NPQ1*::*NPQ1 5′-UTR*-Luc construct, however, increased ~2.5-fold in *eifiso4g1/2* leaves relative to WT (Fig. 8*B*). These results suggest that loss of eIFiso4G expression results in reduced *NPQ1* promoter activity but that the *NPQ1* 5′-UTR is required for increasing expression in *eifiso4g1/2* mutant.

To examine whether the increase in luciferase activity from the *NPQ1*::*NPQ1 5′-UTR*-Luc construct was a result of an increase in the Luc transcript level, qPCR of Luc mRNA was performed in the *eifiso4g1/2* and WT lines. Luc transcript level from the *NPQ1*::Luc and 35S::Luc constructs was substantially reduced in *eifiso4g1/2* relative to WT (Fig. 8*C*). In contrast, the level of Luc mRNA from the *NPQ1*::*NPQ1 5′-UTR*-Luc construct was 6.3-fold higher in *eifiso4g1/2* than in WT (Fig. 8*C*). The addition of the *NPQ1* 5′-UTR decreased the transcript level ~3-fold in WT plants, whereas its presence increased transcript level 37-fold in *eifiso4g1/2* (Fig. 8*D*). These results demonstrate that inclusion of the *NPQ1* 5′-UTR is required for the increase in *NPQ1* transcript level following loss of eIFiso4G expression.

DISCUSSION

In this study, we have examined the effect that loss of eIFiso4G expression has on VDE expression and, consequently, on photosynthetic performance. Despite the fact that plants, like other eukaryotes, express two forms of eIF4G, loss of eIFiso4G expression had profound effects on photochemistry that correlated with a substantial reduction in chlorophyll content, an increase in NPQ, a lower rate of growth, and a reduction in biomass accumulation. Similar effects were not observed following loss of eIF4G, suggesting that eIFiso4G is required to support photosynthetic activity and plant growth, whereas eIF4G is less important in this regard. The smaller plant stature of the *eifiso4g1/2* mutant was principally a result of a reduction in cell size with only a small reduction in cell number per leaf. Although the stomatal index (*i.e.* the ratio of stomata per epidermal cell) was little changed in the *eifiso4g1/2* mutant, a substantial reduction in the number of trichomes per leaf was observed, which together with the reduction in leaf size suggested that eIFiso4G expression is required for normal leaf development. The smaller size of the mutant was reflected in its biomass accumulation, which was less than 10% of the WT fresh or dry weight.

Chlorophyll content in the *eifiso4g1/2* mutant was reduced to 79% of the WT level in low light-grown plants. When grown at higher light intensities, the chlorophyll content of WT plants increased, whereas that of the *eifiso4g1/2* mutant did not, suggesting that loss of eIFiso4G expression results in greater photosensitivity. *eifiso4g1/2* plants also exhibited a higher oxidative load that increased disproportionately upon exposure to higher light intensities, which also supports the notion that the *eifiso4g1/2* mutant experiences increased photosensitivity.

The reduction in chlorophyll content in *eifiso4g1/2* leaves was accompanied by a significant reduction in photosynthetic activity as measured by the net rate of CO_2 assimilation, which likely contributed to its reduced biomass accumulation. *eifiso4g1/2* plants did not exhibit an increase in photorespiration, and the observed small increase in dark respiration could not account for the substantial reduction in photosynthetic activity or biomass accumulation. Similarly, an increase in the level of Rubisco could not account for the reduced photosynthetic activity in the *eifiso4g1/2* mutant because a similar increase in Rubisco in the *eif4g/eifiso4g1* mutant did not affect its photosynthetic activity.

Although loss of eIFiso4G expression did result in reduced stomatal conductance, it was insufficient to account for the lower rate of CO_2 assimilation because the substomatal CO_2 concentration was not reduced. The *eifiso4g1/2* mutant, however, did exhibit elevated induction of NPQ, which included increases in the qE and qI components of NPQ. Because NPQ competes with photosynthesis for absorbed light energy, this increase in NPQ in the *eifiso4g1/2* mutant likely contributes to its lower photosynthetic activity. Indeed, simultaneous measurements of the quantum efficiency of PSII with the induction of NPQ revealed that the quantum efficiency of PSII in *eifiso4g1/2* plants was inversely correlated with NPQ and was

reduced substantially relative to the wild type, whereas NPQ was elevated.

Although an increase in the qI component of NPQ was consistent with the increased photosensitivity of *eifiso4g1/2* as measured by an increase in ROS production and a decrease in relative chlorophyll content, the increase in the qE component suggested an increase in one or more of those factors that contribute to qE. Although expression of PsbS, which is required for qE, was unchanged in *eifiso4g1/2* leaves, an increase in the xanthophyll de-epoxidation state was observed following exposure to light. This suggested an increase in the level of VDE expression and/or activity.

VDE undergoes activation following exposure to light as a result of the light-driven proton pumping across the thylakoid membrane that causes acidification of the thylakoid lumen (35). VDE can be fully activated in isolated thylakoids by the pH of the buffer, and this reflects the maximum capacity of VDE activity present in the thylakoids. In this assay, the *eifiso4g1/2* mutant exhibited a 2-fold higher level of VDE activity relative to WT, which correlated with increases in the VDE protein and transcript levels and a higher de-epoxidation state in light-treated leaves. Because no change in ZE activity, which catalyzes the reverse reaction of VDE, was observed, these results indicate the effect that the loss of eIFiso4G expression has on the xanthophyll cycle is specific to VDE expression. The increase in VDE expression explains the increase in the de-epoxidation state in the *eifiso4g1/2* leaves and its faster initial induction of NPQ in response to light exposure. The higher level of qI in *eifiso4g1/2* leaves suggests that despite the higher level of zeaxanthin and qE, the *eifiso4g1/2* mutant is unable to prevent an increase in qI, an increase in ROS production, and a reduction in chlorophyll.

The increased *NPQ1* transcript level in *eifiso4g1/2* leaves suggested either increased *NPQ1* promoter activity or increased *NPQ1* transcript stability. The reporter assay data argued against an increase in *NPQ1* promoter activity in *eifiso4g1/2* leaves in that when the *NPQ1* promoter was used to drive luciferase expression, a more than 4-fold decrease in luciferase activity was observed in the *eifiso4g1/2* mutant relative to WT plants. This decrease in expression from the *NPQ1* promoter in *eifiso4g1/2* leaves correlated with a substantial decrease in Luc reporter transcript level. Inclusion of the *NPQ1* 5′-UTR in the Luc construct in WT plants decreased Luc activity ~3-fold relative to the construct lacking the *NPQ1* 5′-UTR, correlating with an approximate 4-fold decrease in Luc transcript level. The *NPQ1* 5′-UTR contains two small open reading frames upstream of the VDE coding region. Although small upstream open reading frames can destabilize a transcript through nonsense-mediated decay (36–38), the role of those present in the *NPQ1* 5′-UTR remains to be determined. In contrast to the findings in WT plants, inclusion of the *NPQ1* 5′-UTR actually increased Luc activity in *eifiso4g1/2* leaves, correlating with a 6.3-fold increase in Luc transcript levels, which compared with a 5.28-fold increase in the endogenous level of *NPQ1* mRNA in *eifiso4g1/2* leaves relative to wild-type plants. The observation that the presence of the *NPQ1* 5′-UTR decreased transcript level 3-fold in WT plants (relative to the construct lacking the *NPQ1* 5′-UTR) but increased transcript level 37-fold in *eifiso4g1/2* (relative to the construct lacking the *NPQ1* 5′-UTR) indicates that changes in the expression of eIFiso4G can affect the level of a transcript containing the *NPQ1* 5′-UTR substantially. These results suggest that the increase in VDE expression and activity observed in the *eifiso4g1/2* mutant is a result of the loss of eIFiso4G expression, which increased mRNA levels in a *NPQ1* 5′-UTR-dependent manner.

In the absence of eIFiso4G, an increase in RbcL and a reduction in light-harvesting complex II were also observed, demonstrating that loss of eIFiso4G expression affects more than just VDE expression. Therefore, loss of eIFiso4G likely affects the expression of several components of the photosynthetic machinery that may contribute to the *eifiso4g1/2* phenotype. The present findings indicate that, with regard to the xanthophyll cycle, eIFiso4G is required to support the appropriate level of VDE expression.

Although eIFiso4G and eIF4G interact with similar partner proteins, such as eIF4E, eIF4A, eIF4B, eIF3, and PABP (24, 39), and both function to promote protein synthesis, mRNAs exhibit clear preferences between eIFiso4G and eIF4G for their translation (25–27), which may be a consequence of their substantial differences in size, sequence, and manner of interaction with partner proteins (22, 24, 39). Loss of either initiation translation factor would be predicted to affect the expression of many genes. Despite the functional differences between eIFiso4G and eIF4G, eIFiso4G must be able to compensate for the loss of eIF4G because the *eif4g* null mutant exhibits no obvious mutant phenotype, at least under normal growth conditions. The reduced photochemistry and pale green phenotype of the *eifiso4g* null mutant that are not evident in the *eif4g* null mutant suggest that eIF4G is unable to compensate fully for the loss of eIFiso4G. Consequently, loss of eIFiso4G results, in aberrantly high levels of VDE expression and xanthophyll de-epoxidation, elevated induction of NPQ, reduced photochemistry, lower chlorophyll content, and reduced growth rate, stature, and biomass accumulation. These phenotypes suggest that genes within specific pathways, such as NPQ1, require eIFiso4G for their correct expression, which eIF4G alone is unable to support.

Acknowledgments—We thank Dr. Karen Browning for providing the initiation factor mutant lines, Dr. Krishna Niyogi for the gift of the anti-PsbS antiserum, and Dr. Tadahiko Mae for the gift of the anti-Rubisco antiserum.

REFERENCES

1. Asada, K., and Takahashi, M. (1987) Production and scavenging of active oxygen in photosynthesis. In *Photoinhibition* (Kyle, D. J., Osmond, C. B., and Arntzen, C. J., eds) pp. 227–287, Elsevier, Amsterdam, The Netherlands
2. Niyogi, K. K. (1999) Photoprotection revisited: genetic and molecular approaches. *Annu. Rev. Plant Physiol. Plant Mol. Biol.* **50,** 333–359
3. Aro, E. M., Virgin, I., and Andersson, B. (1993) Photoinhibition of photosystem II. Inactivation, protein damage and turnover. *Biochim. Biophys. Acta* **1143,** 113–134
4. Nishiyama, Y., Allakhverdiev, S. I., and Murata, N. (2006) A new paradigm for the action of reactive oxygen species in the photoinhibition of photosystem II. *Biochim. Biophys. Acta* **1757,** 742–749
5. Demmig-Adams, B., and Adams, W. W., 3rd (1992) Carotenoid composition in sun and shade leaves of plants with different life forms. *Plant Cell Environ.* **15,** 411–419

6. Horton, P., Ruban, A. V., and Walters, R. G. (1996) Regulation of light harvesting in green plants. *Annu. Rev. Plant Physiol. Plant Mol. Biol.* **47,** 655–684
7. Flexas, J., and Medrano, H. (2002) Drought-inhibition of photosynthesis in C3 plants: Stomatal and non-stomatal limitations revisited. *Ann. Bot.* **89,** 183–189
8. Chaves, M. M., Pereira, J. S., Maroco, J., Rodrigues, M. L., Ricardo, C. P., Osório, M. L., Carvalho, I., Faria, T., and Pinheiro, C. (2002) How plants cope with water stress in the field. Photosynthesis and growth. *Ann. Bot.* **89,** 907–916
9. Ramachandra Reddy, A., Chaitanya, K. V., and Vivekanandan, M. (2004) Drought-induced responses of photosynthesis and antioxidant metabolism in higher plants. *J. Plant Physiol.* **161,** 1189–1202
10. Müller-Moulé, P., Golan, T., and Niyogi, K. K. (2004) Ascorbate-deficient mutants of *Arabidopsis* grow in high light despite chronic photooxidative stress. *Plant Physiol.* **134,** 1163–1172
11. Preiss, T., and Hentze, M. (2003) Starting the protein synthesis machine: eukaryotic translation initiation. *BioEssay* **10,** 1201–1211
12. Kapp, L. D., and Lorsch, J. R. (2004) The molecular mechanics of eukaryotic translation. *Annu. Rev. Biochem.* **73,** 657–704
13. Pestova, T. V., Lorsch, J. R., and Hellen, C. U. (2007) The mechanism of translation initiation in eukaryotes. In *Translational Control in Biology and Medicine* (Mathews, M. B., Sonenberg, N., and Hershey, J. W. B., eds) pp. 87–128, Cold Spring Harbor Laboratory Press, Cold Spring Harbor, NY
14. Gallie, D. R. (2002) Protein-protein interactions required during translation. *Plant Mol. Biol.* **50,** 949–970
15. Wei, C.-C., Balasta, M. L., Ren, J., and Goss, D. J. (1998) Wheat germ poly(A) binding protein enhances the binding affinity of eukaryotic initiation factor 4F and (iso)4F for cap analogues. *Biochemistry* **37,** 1910–1916
16. Bi, X., and Ren, J., and Goss, D. J. (2000) Wheat germ translation initiation factor eIF4B affects eIF4A and eIFiso4F helicase activity by increasing the ATP binding affinity of eIF4A. *Biochemistry* **39,** 5758–5765
17. Tarun, S. Z., Jr., and Sachs, A. B. (1995) A common function for mRNA 5′ and 3′ ends in translation initiation in yeast. *Genes Dev.* **9,** 2997–3007
18. Wells, S. E., Hillner, P. E., Vale, R. D., and Sachs, A. B. (1998) Circularization of mRNA by eukaryotic translation initiation factors. *Mol. Cell* **2,** 135–140
19. Le, H., Tanguay, R. L., Balasta, M. L., Wei, C.-C., Browning, K. S., Metz, A. M., Goss, D. J., and Gallie, D. R. (1997) Wheat germ poly(A) binding protein enhances the binding affinity of eukaryotic initiation factor 4F and (iso)4F for cap analogues. *J. Biol. Chem.* **272,** 16247–16255
20. Le, H., Browning, K. S., and Gallie, D. R. (2000) The phosphorylation state of poly(A)-binding protein specifies its binding to poly(A) RNA and its interaction with eukaryotic initiation factor (eIF) 4F, eIFiso4F, and eIF4B. *J. Biol. Chem.* **275,** 17452–17462
21. Cheng, S., and Gallie, D. R. (2006) Wheat eukaryotic initiation factor 4B organizes assembly of RNA and eIFiso4G, eIF4A, and poly(A)-binding protein. *J. Biol. Chem.* **281,** 24351–24364
22. Gallie, D. R., and Browning, K. S. (2001) eIF4G functionally differs from eIFiso4G in promoting internal initiation, cap-independent translation, and translation of structured mRNAs. *J. Biol. Chem.* **276,** 36951–36960
23. Browning, K. S. (1996) The plant translational apparatus. *Plant Mol. Biol.* **32,** 107–144
24. Cheng, S., and Gallie, D. R. (2013) Eukaryotic initiation factor 4B and the poly(A)-binding protein bind eIF4G competitively. *Translation* **1,** e24038
25. Gallie, D. R. (2002) The 5′-leader of tobacco mosaic virus promotes translation through enhanced recruitment of eIF4F. *Nucleic Acids Res.* **30,** 3401–3411
26. Gallie, D. R. (2001) Cap-independent translation conferred by the 5′-leader of tobacco etch virus is eIF4G-dependent. *J. Virol.* **75,** 12141–12152
27. Mayberry, L. K., Allen, M. L., Dennis, M. D., and Browning, K. S. (2009) Evidence for variation in the optimal translation initiation complex: plant eIF4B, eIF4F, and eIF(iso)4F differentially promote translation of mRNAs. *Plant Physiol.* **150,** 1844–1854
28. Lellis, A. D., Allen, M. L., Aertker, A. W., Tran, J. K., Hillis, D. M., Harbin, C. R., Caldwell, C., and Gallie, D. R., Browning, K. S. (2010) Deletion of the eIFiso4G subunit of the *Arabidopsis* eIFiso4F translation initiation complex impairs health and viability. *Plant Mol. Biol.* **74,** 249–263
29. Jeffrey, S. W., and Humphrey, G. F. (1975) New spectrophotometric equations for determining chlorophylls *a*, *b*, *c*1 and *c*2 in higher plants, algae, and natural phytoplankton. *Biochem. Physiol. Pflanz* **167,** 191–194
30. Gilmore, A. M., and Yamamoto, H. Y. (1991) Zeaxanthin formation and energy-dependent fluorescence quenching in pea chloroplasts under artificially mediated linear and cyclic electron transport. *Plant Physiol.* **96,** 635–643
31. Maxwell, K., and Johnson, G. N. (2000) Chlorophyll fluorescence: a practical guide. *J. Exp. Bot.* **51,** 659–668
32. Gay, C. A., and Gebicki, J. M. (2002) Perchloric acid enhances sensitivity and reproducibility of the ferric-xylenol orange peroxide assay. *Anal. Biochem.* **304,** 42–46
33. Havaux, M., and Niyogi, K. K. (1999) The violaxanthin cycle protects plants from photooxidative damage by more than one mechanism. *Proc. Natl. Acad. Sci. U.S.A.* **96,** 8762–8767
34. Havaux, M., Gruszecki, W. I., Dupont, I., and Leblanc, R. M. (1991) Increased heat emission and its relationship to the xanthophyll cycle in pea leaves exposed to strong light stress. *J. Photochem. Photobiol. B Biol.* **8,** 361–370
35. Hager, A. (1969) Lichtbedingte pH-Erniedrigung in einem Chloroplasten-Kompartiment als Ursache der enzymatischen Violaxanthin-Zeaxanthin-Umwandlung; Beziehungen zur Photophosphorylierung. *Planta* **89,** 224–243
36. Saul, H., Elharrar, E., Gaash, R., Eliaz, D., Valenci, M., Akua, T., Avramov, M., Frankel, N., Berezin, I., Gottlieb, D., Elazar, M., David-Assael, O., Tcherkas, V., Mizrachi, K., and Shaul, O. (2009) The upstream open reading frame of the *Arabidopsis* AtMHX gene has a strong impact on transcript accumulation through the nonsense-mediated mRNA decay pathway. *Plant J.* **60,** 1031–1042
37. He, F., Li, X., Spatrick, P., Casillo, R., Dong, S., and Jacobson, A. (2003) Genome-wide analysis of mRNAs regulated by the nonsense-mediated and 5′ to 3′ mRNA decay pathways in yeast. *Mol. Cell* **12,** 1439–1452
38. Mendell, J. T., Sharifi, N. A., Meyers, J. L., Martinez-Murillo, F., and Dietz, H. C. (2004) Nonsense surveillance regulates expression of diverse classes of mammalian transcripts and mutes genomic noise. *Nat. Genet.* **36,** 1073–1078
39. Cheng, S., and Gallie, D. R. (2010) Competitive and noncompetitive binding of eIF4B, eIF4A, and the poly(A) binding protein to wheat translation initiation factor eIFiso4G. *Biochemistry* **49,** 8251–8265